

Supporting Information for: DART-MS analysis of inorganic explosives using high temperature thermal desorption

Thomas P. Forbes*, Edward Sisco, Matthew Staymates, and Greg Gillen

National Institute of Standards and Technology, Materials Measurement Science Division, Gaithersburg, MD, USA

* Corresponding author: E-mail: thomas.forbes@nist.gov; Tel: 1-301-975-2111

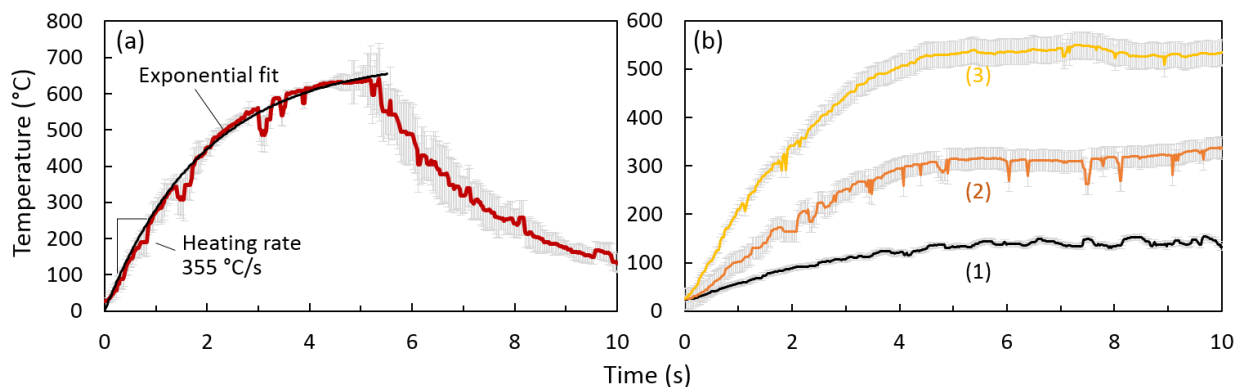


Figure S1. Transient nichrome wire temperature measurements for (a) 5.5 s pulse of 3.13 A current and (b) steady state temperatures for 0.83 A, 1.52 A, and 2.34 A current. Data and uncertainty represent the average and standard deviation ($k=1$) of triplicate measurements. Black curve in (a) represents MATLAB fitted exponential function.

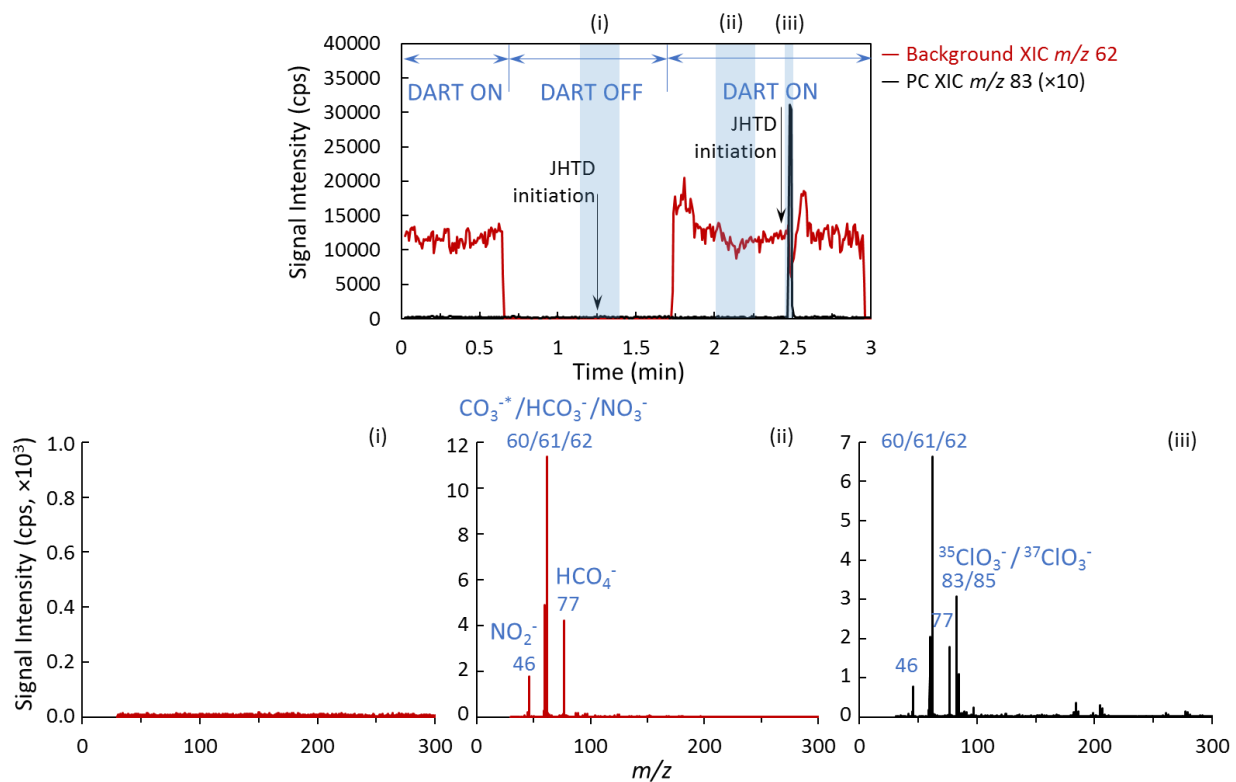


Figure S2. JHTD-DART-MS extracted ion chromatograms (XICs) for the background nitrate (m/z 62) signal and 100 ng PC (m/z 83) with the DART voltages OFF and ON. (i)-(iii) Extracted mass spectra from respective locations denoted by blue boxes in the chronograms.

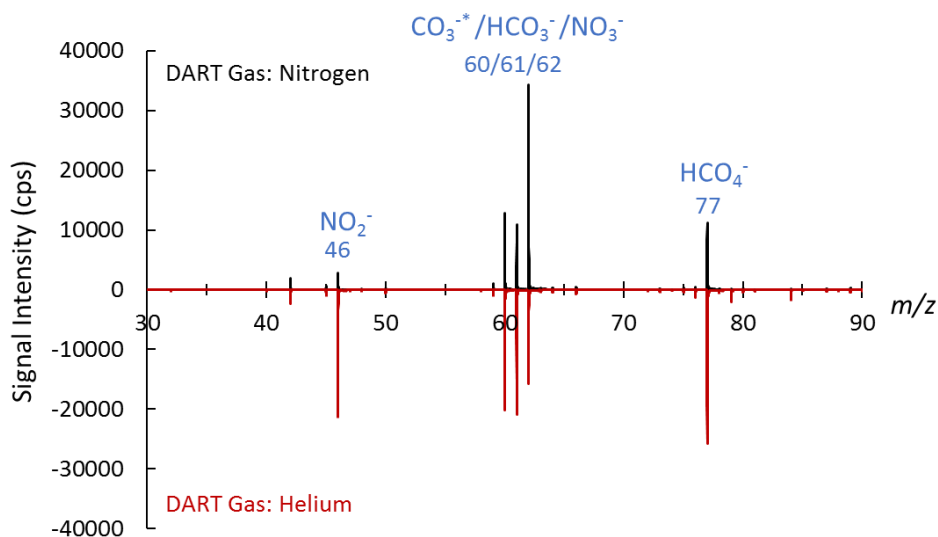


Figure S3. Representative DART generated background mass spectra for nitrogen (top) and helium (bottom) under negative mode operation and 200 °C gas stream temperature – JHTD wire present with no heating.

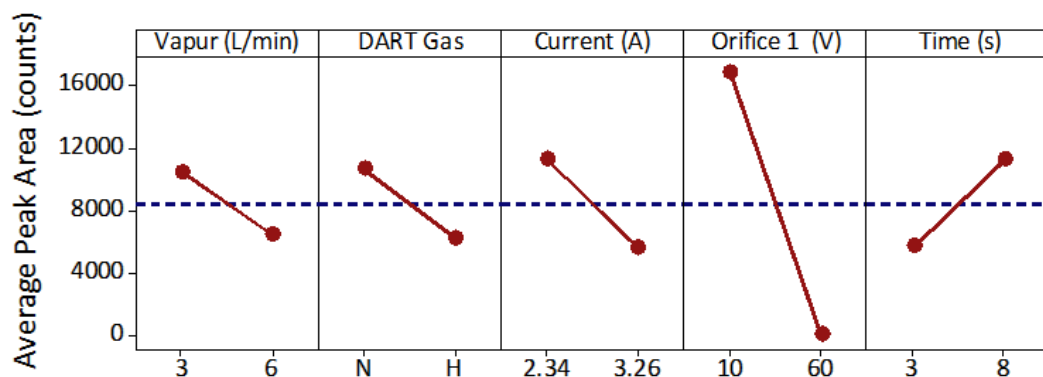


Figure S4. JHTD-DART-MS main effects plot for the partial factorial DOE of five factors: Vapor flow rate (Vapor), DART ionization gas (DART Gas), nichrome wire current (Current), orifice 1 voltage/in-source CID (Orifice 1), and current pulse duration (Time) for 100 ng deposits of pentaerythritol tetranitrate (PETN).

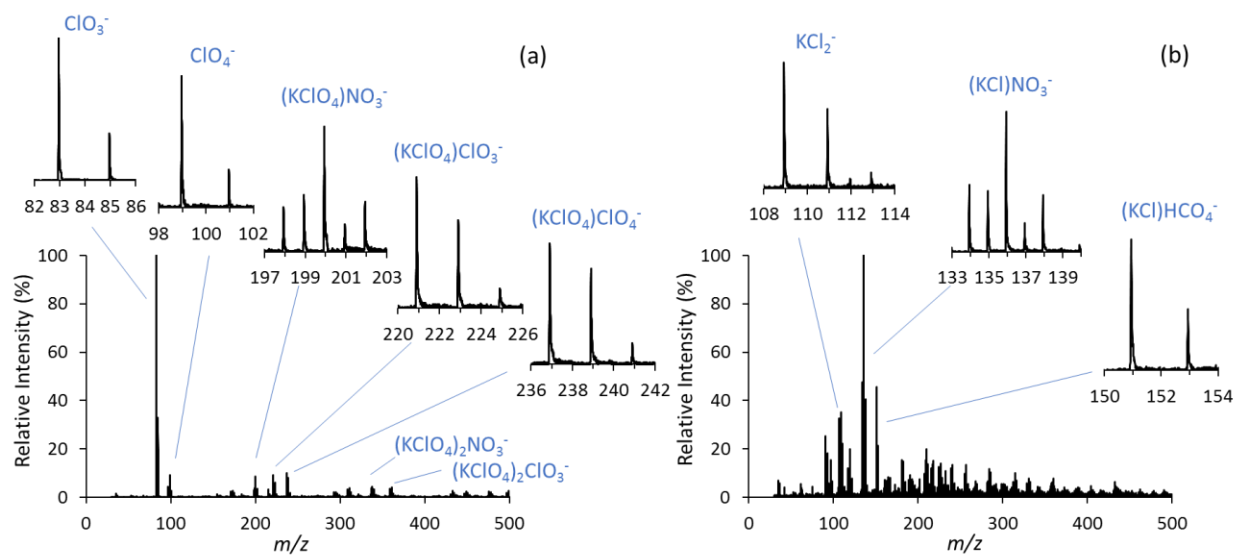


Figure S5. JHTD-DART-MS mass spectra corresponding to sequential time points for the detection of the (a) PPC desorption products and (b) PPC decomposition products (100 ng PPC sample and 3.13 A).

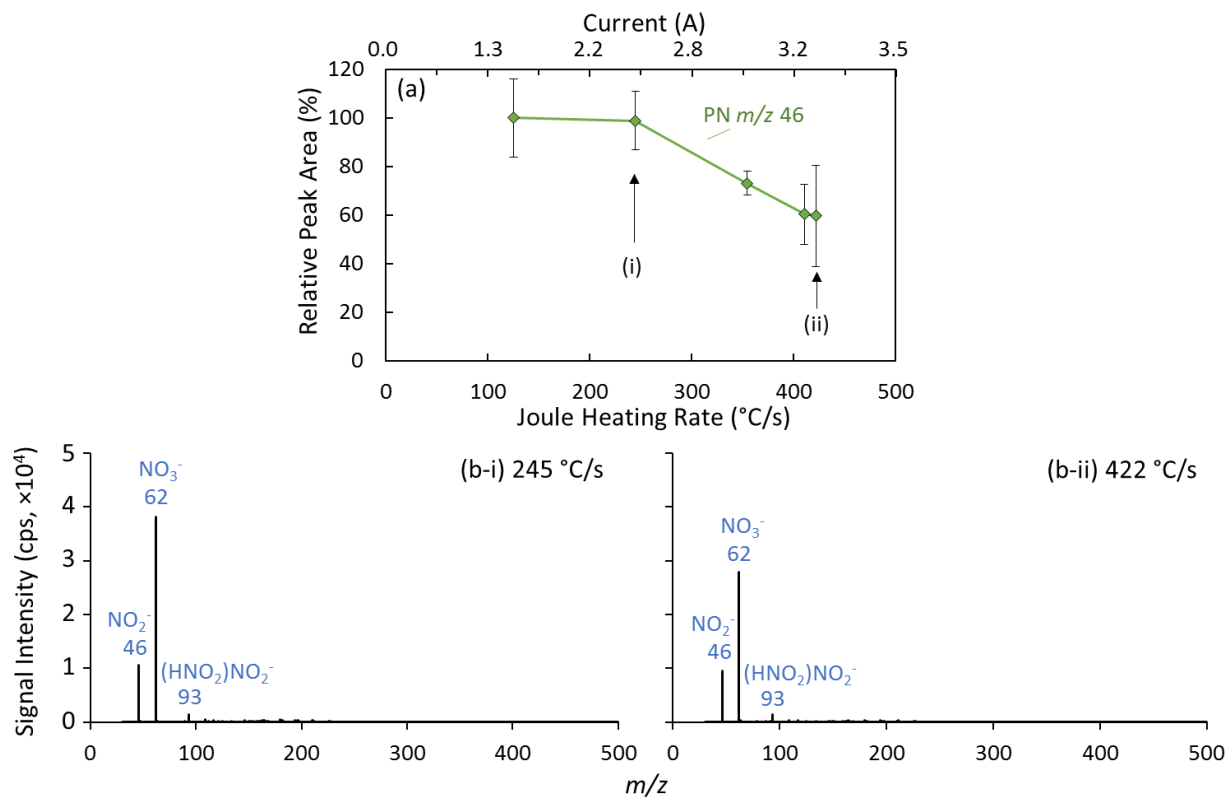


Figure S6. (a) JHTD-DART-MS normalized integrated peak area for the nitrite monomer from 100 ng PN (m/z 46, NO_2^- , \blacklozenge) samples as a function of passed current and heating rate. (b) Representative spectra of PN for heating rates of (b-i) 245 $^{\circ}\text{C}/\text{s}$ and (b-ii) 422 $^{\circ}\text{C}/\text{s}$. Data points and uncertainty expressed as the average peak area and standard deviation ($k=1$) derived from XICs for five replicate measurements.

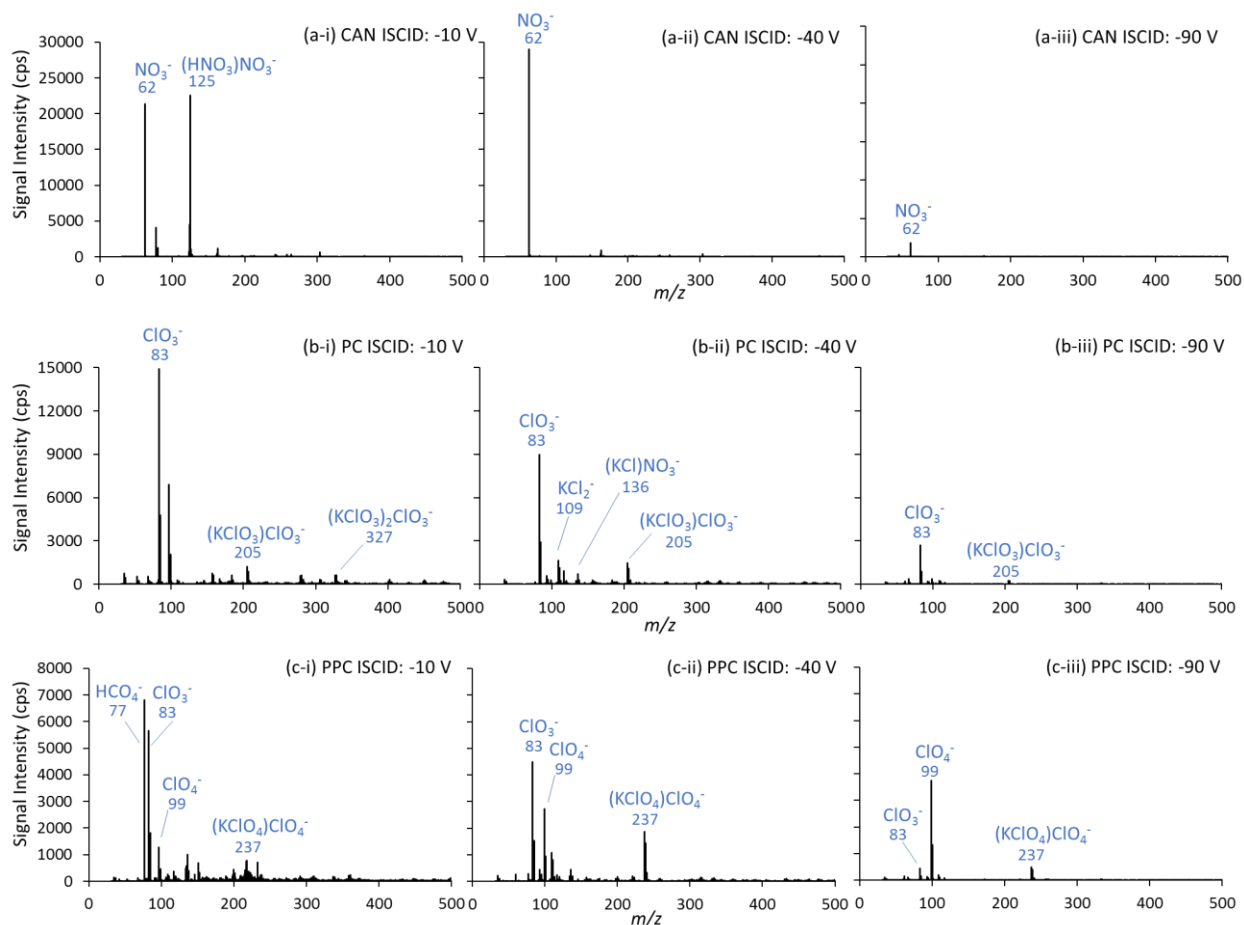


Figure S7. Representative background subtracted JHTD-DART mass spectra as a function of in-source collision induced dissociation for (a) CAN, (b) PC, and (c) PPC.

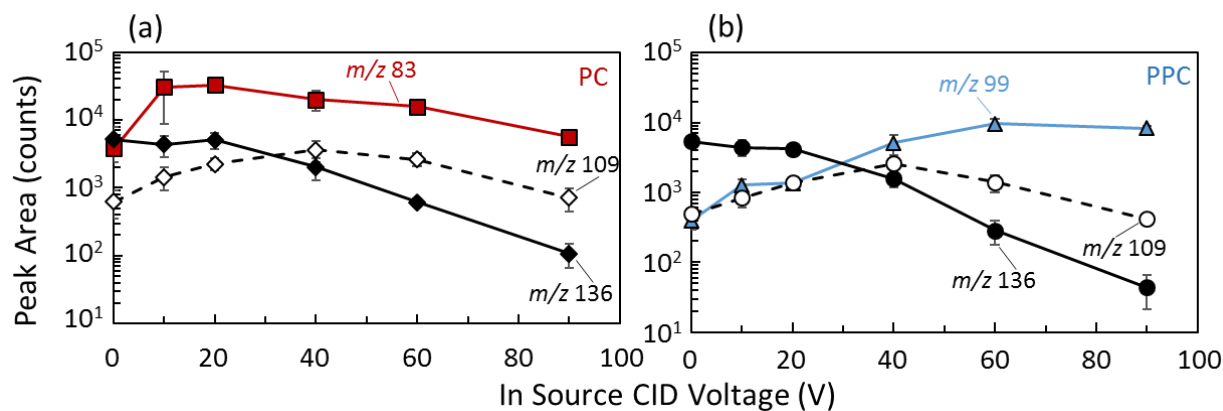


Figure S8. JHTD-DART-MS integrated peak area as a function of in-source collision induced dissociation (CID) voltage for 100 ng samples of the molecular anion and thermal decomposition species for (a) PC and (b) PPC. PC: m/z 83, ClO_3^- , \blacksquare —, m/z 109, KCl_2^- , \blacklozenge —, m/z 136, $(\text{KCl})\text{NO}_3^-$, \blacklozenge —; PPC: m/z 99, ClO_4^- , \blacktriangle —, m/z 109, KCl_2^- , \blacklozenge —, m/z 136, $(\text{KCl})\text{NO}_3^-$, \blacklozenge —.

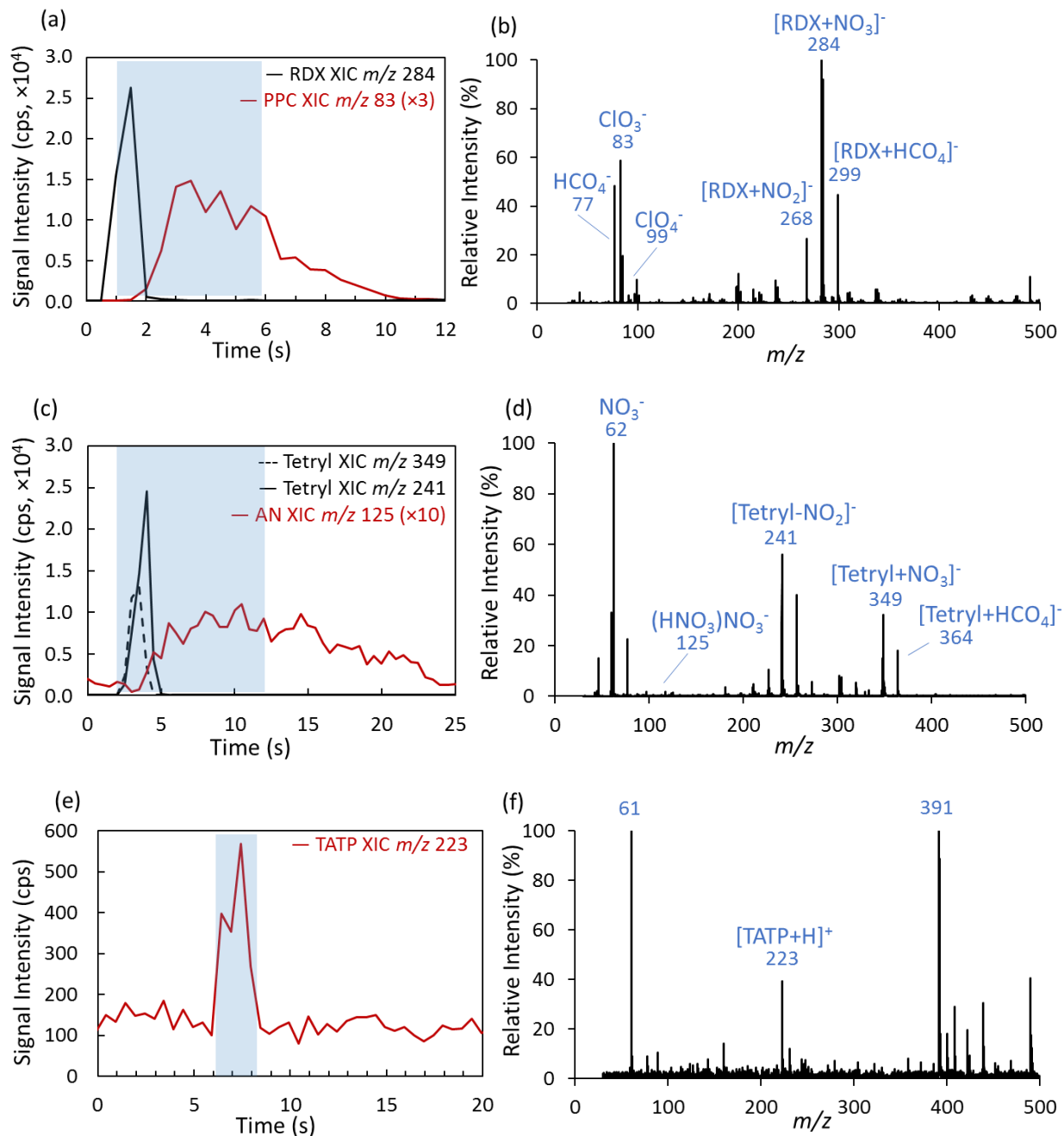


Figure S9. JHTD-DART-MS extracted ion chromatograms (XICs) for (a) a mixture of 100 ng each of RDX and PPC at a heating rate and maximum temperature of 245 °C/s and 536 °C, (c) a mixture of 100 ng each of Tetryl and AN at a heating rate and maximum temperature of 125 °C/s and 355 °C, and (e) a mixture of 200 ng each of TATP and CAN at a heating rate and maximum temperature of 125 °C/s and 355 °C. (b), (d), and (f) Extracted mass spectra from respective locations denoted by blue boxes in the chromatograms (a), (c), and (e).